BNL 38425

COLLAPSE OF ACCRETING CARBON-OXYGEN WHITE DWARFS INDUCED BY CARBON DEFLAGRATION AT HIGH DENSITY

BNL--38425

DE86 015076

Ken'ichi Nomoto [1]

Department of Physics, Brookhaven National Laboratory
Upton, NY 11973, U.S.A.

ABSTRACT

We have obtained a critical condition for which carbon deflagration induces collapse of a accreting C+O white dwarf, not explosion. If the carbon deflagration is initiated at central density as high as 10^{10} g cm^{-3} and if the propagation of the deflagration wave is slower than $\sim 0.15\ v_s$ (v_s is the sound speed), electron capture behind the burning front induces collapse to form a neutron star. This is the case for both conductive and convective deflagrations. Such a high central density can be reached if the white dwarf is sufficiently massive and cold at the onset of accretion and if the accretion rate is in the appropriate range. Models for Type Ia and Ib supernovae are also discussed.

to appear in Proceedings of XXIth Rencontre de Moriond
VIth Astrophysics Meeting
ACCRETION PROCESSES IN ASTROPHYSICS
March 9 - 15, 1986, Les Arcs, France

---

[1] On leave from the Department of Earth Science and Astronomy, College of Arts and Sciences, University of Tokyo, Meguro-ku, Tokyo 153, Japan.

1. INTRODUCTION

The final fate of accreting white dwarfs has attracted a lot of recent attention because it is related to the origin of Type I supernovae and low mass X-ray binaries. In fact, the exploding white dwarf model for Type I supernovae, in particular, the carbon deflagration model is in good agreement with many of the observations.[1,2] Such success implies that at least some accreting white dwarfs increase their mass to the Chandrasekhar mass, though the exact evolution of the binary systems leading to the supernova stage is not yet known.

Recent observations of several interesting binary systems, low mass X-ray binaries, QPOs, and binary radio pulsars have suggested that in these systems a neutron star has formed from accretion-induced collapse of a white dwarf.[3,4]

Possible models for the white dwarf collapse involve solid C+O white dwarfs, in which carbon and oxygen may or may not have chemically separated [5,6] and O+Ne+Mg white dwarfs.[7] For a wide range of mass accretion rates and initial white dwarf masses, the O+Ne+Mg white dwarfs collapse due to electron capture on ^{24}Mg and ^{20}Ne.[8,9] On the other hand, depending on the conditions of the white dwarfs and binary systems in which they are formed, the C+O white dwarfs could either explode or collapse. Chemical separation in such objects is still hypothetical and in any case could not be complete before carbon burning starts.[10] It takes a carbon fraction of only a few percent to sustain a deflagration.

Therefore, it is worth determining the critical condition for which a carbon deflagration induces the collapse of a C+O white dwarf rather than its explosion. Such a condition has been obtained for the carbon detonation,[11] but not for the carbon deflagration except for the pulsation-driven propagation model.[12] We have performed numerical simulations of conductive and convective deflagrations starting from $\rho_c \sim 10^{10}$ g cm^{-3} and found that the C+O white dwarf collapses if the propagation velocity is slower than $\sim 0.15\, v_s$ (v_s is the sound speed). Generally, for both conductive and convective deflagrations, this is the case.

2. THE EVOLUTION OF WHITE DWARFS AS A FUNCTION OF ACCRETION RATE

Isolated white dwarfs are simply cooling stars that eventually end up as *dark matter*. In binary systems they evolve differently because mass accretion from their companion provides gravitational energy that rejuvenates them. The gravitational energy released at the accretion shock near the stellar surface is radiated away and does not heat the white dwarf interior. However, the compression of the interior by the accreted matter releases additional gravitational energy. Some of this energy goes into thermal energy (compressional heating) and the rest is transported to the surface and radiated away (radiative cooling). Therefore, the interior temperature is determined by the balance between heating and cooling and, thus, strongly depends on the mass accretion rate, $\dot{M}$.[13,14]

Compression first heats up a layer near the surface because of the small pressure scale height there. Later, heat diffuses inward (Fig. 3). The diffusion timescale depends on $\dot{M}$ and is small for larger $\dot{M}$'s because of the large heat flux and steep temperature gradient generated by rapid accretion. For example, the time it takes the heat wave to reache the central region is about 2×10^5 yr for $\dot{M} \sim 10^{-8}\ M_\odot\ \mathrm{yr}^{-1}$ (Fig. 3)[15] and 5×10^6 yr for $\dot{M} \sim 4 \times 10^{-8}\ M_\odot\ \mathrm{yr}^{-1}$.[16] Therefore, more than 0.2 $M_\odot$ of matter has accreted from the companion if the entropy in the center increases due to the heat inflow. In other words, if the initial mass of the white dwarf, M_{CO}, is larger than 1.2 $M_\odot$, the central region is compressed only adiabatically and thus is cold when the white dwarf mass becomes 1.4 $M_\odot$. If the white dwarf is sufficiently massive and cold at the onset of accretion, carbon burning will be ignited in the center when density is as high as 10^{10} g cm^{-3}.[6]

Accordingly, the ultimate fate of accreting C+O white dwarfs depends on $\dot{M}$ and the inintial mass of the white dwarf M_{CO}, as summarized in Figure 1. $\dot{M}$ denotes the growth rate of the C+O white dwarf mass irrespective of the composition of the accreting matter. A similar diagram for the O+Ne+Mg white dwarfs is shown in Figure 2. *Neutron Star* or *NS* in Figure 1 indicates a region of parameter space where neutron star formation by white dwarf collapse is expected. The evolution of the white dwarfs in these three regions is summarized as follows:

1) For $\dot{M} > 2.7 \times 10^{-6}\ M_\odot\ \mathrm{yr}^{-1}$, off-center carbon burning is ignited by rapid compressional heating.[15] The C+O white dwarf is peacefully changed into an O+Ne+Mg white

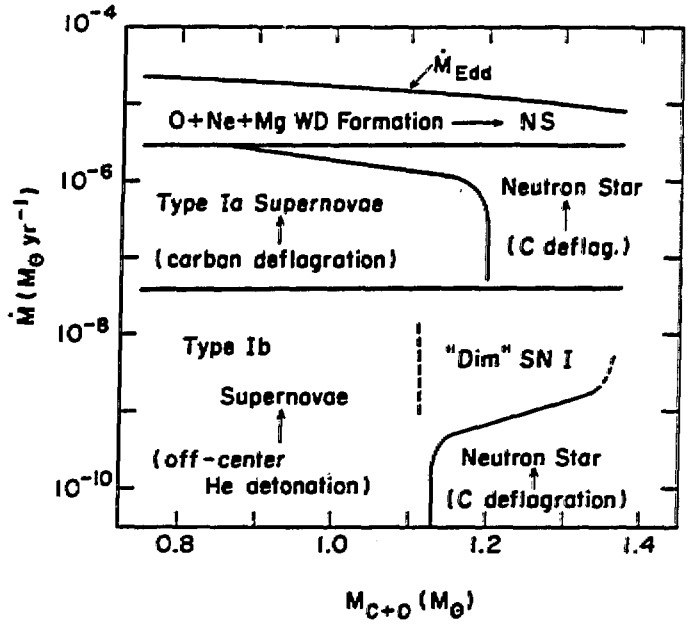

Figure 1: The final fate of accreting C+O white dwarfs expected for their initial mass M_{CO} and accretion rate $\dot{M}$. For two regions in $\dot{M}$ - M_{CO} plane indicated by *Neutron Star*, carbon deflagration is ignited in the center when the density is as high as $\rho_c \simeq 10^{10}$ g cm^{-3}. Propagation of the deflagration wave will induce collapse to form a neutron star. See text for other cases.

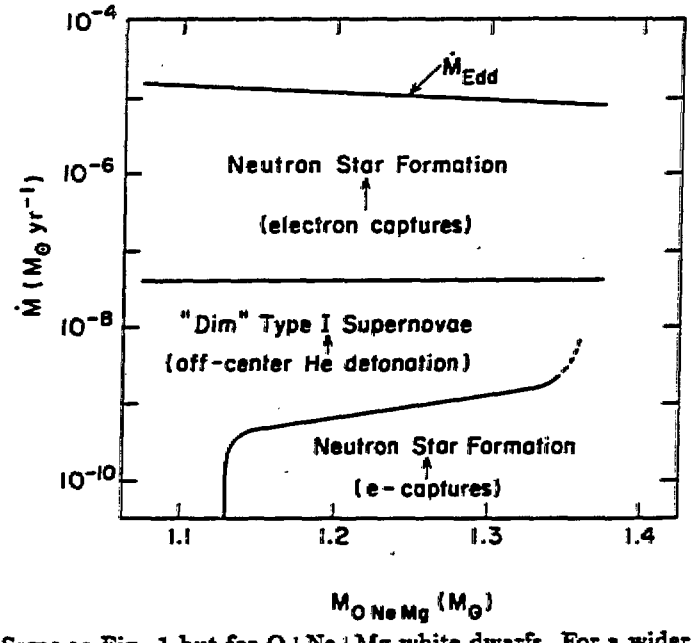

Figure 2: Same as Fig. 1 but for O+Ne+Mg white dwarfs. For a wider range of $\dot{M}$ and the initial mass, M_{ONeMg}, neutron star formation triggered by electron capture on ^{24}Mg and ^{20}Ne is expected.

dwarf through off-center carbon burning.[17,18] The resulting O+Ne+Mg white dwarf will collapse to form a neutron star if the Chandrasekhar mass is reached.[7]

2) For $2.7 \times 10^{-6}\ M_\odot\ \mathrm{yr}^{-1} > \dot{M} > 4 \times 10^{-8}\ M_\odot\ \mathrm{yr}^{-1}$ and $M_{\mathrm{CO}} > 1.2\ M_\odot$, a central density as high as 10^{10} g cm^{-3} is reached by adiabatic compression if the white dwarf is sufficiently cold at the onset of accretion.[19] For $\dot{M} > 10^{-6}\ M_\odot\ \mathrm{yr}^{-1}$, the lower mass limit is not $1.2\ M_\odot$, but $1.0\ M_\odot$.[15] An example of such an evolution is given in Figure 3, where $\dot{M} = 2 \times 10^{-6}\ M_\odot\ \mathrm{yr}^{-1}$.[15]

3) For $\dot{M} \leq 10^{-9}\ M_\odot\ \mathrm{yr}^{-1}$ and $M_{\mathrm{CO}} > 1.13\ M_\odot$, the white dwarf is too cold to initiate a helium detonation.[13,20,21] Eventually pycnonuclear carbon burning starts in the center when ρ_c reaches $\sim 10^{10}$ g cm^{-3}. An evolutionary path of ρ_c - T_c for a model with $\dot{M} = 2.5 \times 10^{-10}\ M_\odot\ \mathrm{yr}^{-1}$ and $M_{\mathrm{CO}} = 1.16\ M_\odot$ is shown in Figure 4. In this model, the outer layer of $0.24\ M_\odot$ is composed of helium.

The fate of white dwarfs in other regions in Figure 1 is described in §3, numerical simulations of carbon deflagrations initiated at high densities are discussed in §4, and in §5 we make some concluding remarks.

3. MODELS FOR SUPERNOVAE OF TYPE Ia AND Ib

3.1 Type Ia Supernovae

For relatively high accretion rates ($2.7 \times 10^{-6}\ M_\odot\ \mathrm{yr}^{-1} > \dot{M} > 4 \times 10^{-8}\ M_\odot\ \mathrm{yr}^{-1}$), a carbon deflagration starts in the white dwarf's center at a relatively low central density ($\rho_c \sim 3 \times 10^9$ g cm^{-3}).[16] The *convective* deflagration wave then propagates outward at a subsonic velocity and incinerates the material of the inner layers to nuclear statistical equilibrium (NSE). When the deflagration wave arrives at the outer layers ($M_r > 0.7\ M_\odot$), the density it then encounters has already decreased below 10^8 g cm^{-3} due to the expansion of the white dwarf. At such densities, the peak temperature attained behind the deflagration front is too low to process the material to NSE. The products of explosive nucleosynthesis depend on the temperature and density at the deflagration front and, thus, vary from layer to layer. In the center, iron peak elements are produced. In particular, about $0.6\ M_\odot$ of ^{56}Ni is synthesized. In the outer layers, intermediate mass elements such as Ca, Ar, S, Si are produced. The white dwarf is disrupted completely and no neutron star residue remains.[16,22]

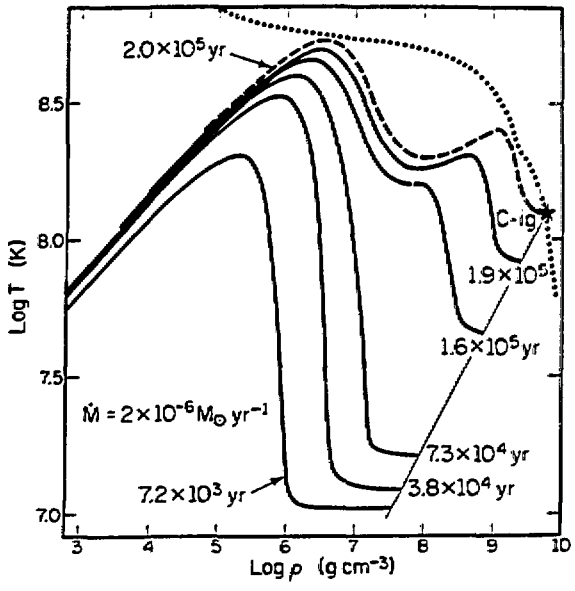

Figure 3: Structure of the accreting C+O white dwarf in the density - temperature plane as a function of time for the model with $\dot{M} = 2 \times 10^{-6}\ M_\odot\ \mathrm{yr}^{-1}$ and $M_{CO} = 1.0\ M_\odot$.[15] A heat wave propagates from the hot outer layer to the central region. Carbon burning is ignited at relatively high central density before the center is heated up. The thin solid lines shows the adiabat followed by the central point for an initial temperature of 10^7 K. For lower (higher) initial temperature, the ignition density is higher (lower) as far as the heat wave does not reach the center. The dotted curve is an approximate ignition line of carbon burnig defined in Fig. 4.

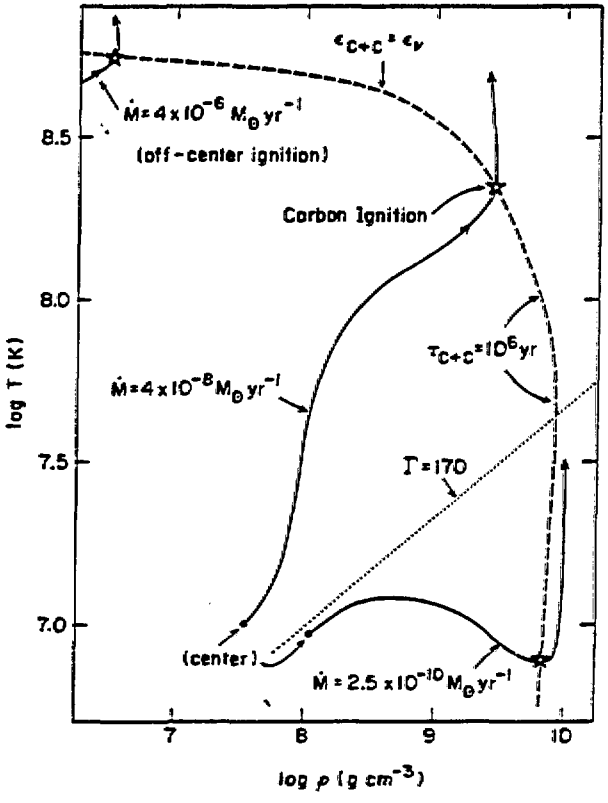

Figure 4: Evolutionary path of (ρ_c, T_c) at the center of accreting C+O white dwarfs for two cases. For $\dot{M} = 4 \times 10^{-8}\ M_\odot\ \mathrm{yr}^{-1}$, carbon deflagration is ignited at relatively low density ($\rho_c \simeq 3 \times 10^9$ g cm^{-3}). This model is in good agreement with many of the observed features of Type Ia supernovae. For $\dot{M} = 2.5 \times 10^{-10}\ M_\odot\ \mathrm{yr}^{-1}$, carbon burning is ignited in the *solid* core ($\Gamma > 170$: below the dotted line) when the central density is as high as $\rho_c \sim 10^{10}$ g cm^{-3}. For comparison, the ignition point of off-center carbon burning is shown for $\dot{M} = 4 \times 10^{-6}\ M_\odot\ \mathrm{yr}^{-1}$.[15] The dashed curve is an approximate ignition line where the rate of carbon burning ϵ_{C+C} is equal to the rate of neutrino losses ϵ_ν for $T > 2 \times 10^8$ K and $\tau_{C+C} \equiv c_p\ T\ /\epsilon_{C+C} = 10^6$ yr for $T \leq 2 \times 10^8$ K (c_p is the specific heat).

The carbon deflagration model can account for the light curves, early time specta, and late time spectra of Type Ia supernovae as follows:[1,2]

1) The theoretical light curve based on the radioactive decays of ^{56}Ni and ^{56}Co into ^{56}Fe fits the observations well.[2,23,24]

2) The synthetic spectum at maximum light is in excellent agreement with the observed spectum of SN 1981b [25] as seen in Figure 5.[26,27,39] The feature near 6125 Å is clearly identified as the Si II line that is a sigature of Type Ia supernovae (see discussion concerning Type Ib below).

3) At late times, the outer layers are transparent and the inner Ni-Co-Fe core is exposed. Synthetic spectra of emission lines of [Fe II] and [Co I] agree quite well with the spectra observed at such phase.[22]

Therefore, there is good evidence that Type I supernovae are exploding white dwarfs.

3.2 Type Ib Supernovae

Recent observations indicate that there exists another kind of Type I supernovae, designated Type Ib (SN Ib).[28-32] The SN Ib spectra lack hydrogen lines (definition of SN I) and are characterized by both the lack of the 6125 Å Si feature at maximum-light spectra and the appearance of oxygen emission lines at late times.[32,33] More than 5 $M_{\odot}$,[34] and as much as 15 $M_{\odot}$,[32] of oxygen has been inferred from the late time spectra. These signatures have led to the currently popular idea that the progenitors of SN Ib are Wolf-Rayet stars.[28,32-35] However, such a large mass of oxygen may yield a theoretcal light curve whose decline is too slow to be compatible with SN Ib observations.[28,36] In addition, Wolf-Rayet death rates and the SN Ib frequency might be incompatible.[28]

Branch and Nomoto [38] have suggested that the observed spectra are better explained by an accreting white dwarf model. In Figure 6, the maximum-light spectrum of SN 1984I[28] is compared with a synthetic spectrum. The expansion velocity of matter at the photosphere is assumed to be 8,000 km s^{-1}. Two of the absorption lines in the red are identified as He I lines [39] and other features are well explained as Fe II lines. In addition, ultraviolet features can fit with a synthetic spectrum of Co II and Fe I lines if the photoshperic velocity is 12,000 km s^{-1}.[40] The above interpretation of the early spectrum together with the presence of the oxygen lines in the late time spectrum suggests that Fe,

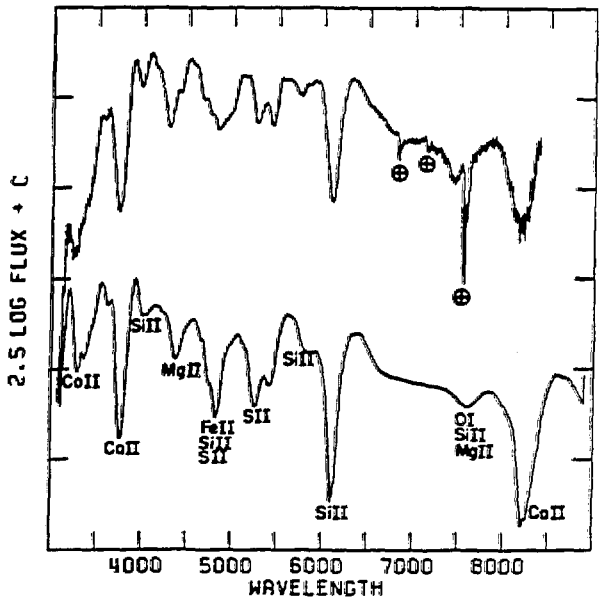

Figure 5: The maximum-light spectrum of SN 1981b (top)[25] is compared to a synthetic spectrum for the carbon deflagration model[16] 15 days after the explosion.[26] In this model outer layer is assumed to be mixed. Terrestrial absorption features in the observed spectrum are indicated.

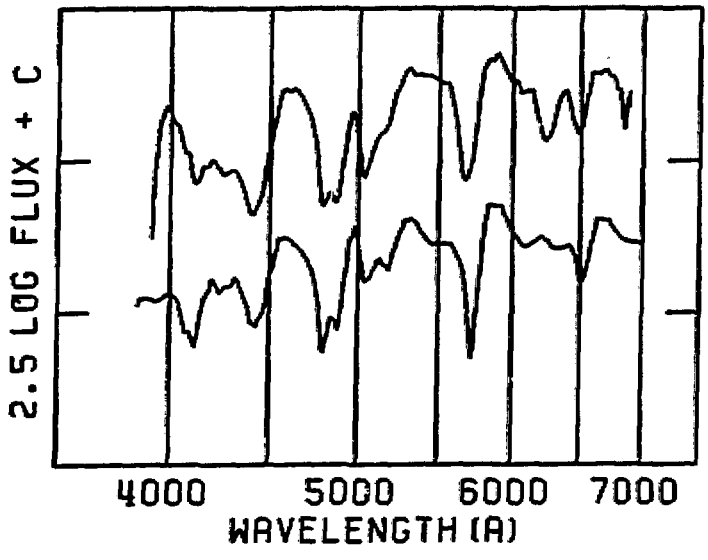

Figure 6: The maximum-light spectrum of the Type Ib SN 1984*I* in NGC 991 (upper)[28] is compared with a synthetic spectrum (lower) based on resonant-scattering lines of He I and Fe II superimposed on a continuum.[38] In the synthetic spectrum the blueshifted absorption component of He I λ6678 appears near 6500 Å and He I λ5876 appears near 5850 Å. Other features are produced primarily by Fe II lines.

Co (decaying), and He are in the outer high-velocity layers and that oxygen and some other intermediate mass elements are in the inner layers. In other words, the composition structure of SN Ib's appears to be that for SN Ia's inverted.

The existence of such high velocity Fe and Co is difficult to explain with the Wolf-Rayet model. Branch and Nomoto [38] have speculated that the progenitors of SN Ib differ from the progenitors of SN Ia in having a lower accretion rate, i.e., $\dot{M} < 4 \times 10^{-8}\ M_\odot$ yr^{-1}. For such low accretion rates, the helium shell flash grows into a detonation. The outcome may be more like a *single* detonation than the double detonation obtained in the spherical calculations [41,42] because the off-center flash will occur at a point rather than all over a spherical shell. The outer helium layer will burn to mostly ^{56}Ni with a trace He and be ejected into space. The inner C+O core will remain unburned due to non-spherical effects and a part or most of the C+O will be ejected. Since the ejected mass of ^{56}Ni will be as small as 0.1 - 0.3 $M_\odot$, the peak luminosity of this model is lower than that for SN Ia by a factor of 2 - 6. This result is consisttent with the observations of SN Ib.[28-31]

This *single* detonation scenario requires that $\dot{M}$ be lower than that needed for the carbon deflagration model of SN Ia. This requirement may be inconsistent with the fact that SN Ib have been seen in only spiral galaxies, usually in their star-forming regions. However, if the white dwarf accretes matter with an efficiency of only 0.03 - 0.1 [43] from a wind (10^{-6} - $10^{-7}\ M_\odot$ yr^{-1}) of a relatively massive (4 - 7 $M_\odot$) red giant companion,[44] the model would be consistent. Further, this scenario is consistent with the radio observations of SN Ib in that they can be explained by the interaction of supernova ejecta with the circumstellar shell.[31,45,46]

Both Wolf-Rayet and white dwarf models for SN Ib should be tested by quantitative comparison with observations based on theoretical light curves, synthetic spectra, and multi-dimensional hydrodynamical calculatons of off-center detonations.

3.3 *Dim* Type I Supernovae

If an off-center *single* detonation occurs on a very massive white dwarf ($> \sim 1.1\ M_\odot$), the resulting supernova will be rather *dim*, because the accumulation of only a small amount of helium ($\sim$ 0.01 - 0.1 $M_\odot$) can lead to the helium detonation.[21] In most cases, an unburned C+O core will be left behind as a white dwarf. Such dim supernovae [47] are more likely to be associated with O+Ne+Mg white dwarfs since their masses are larger than $\sim 1.2\ M_\odot$ (see §5).

4. COLLAPSE INDUCED BY CARBON DEFLAGRATION AT HIGH DENSITY

4.1 Conductive Deflagration

As mentioned in §2, there are two scenarios in which a carbon deflagration is initiated in the center when the central density is as high as 10^{10} g cm^{-3}. In one, the accretion rate is lower than 10^{-9} $M_\odot$ yr^{-1} and the initial white dwarf mass, M_{CO}, is larger than 1.13 $M_\odot$. In the other, $\dot{M} > 4 \times 10^{-8}$ $M_\odot$ yr^{-1} and $M_{CO} > 1.2$ $M_\odot$.

At densities as high as 10^{10} g cm^{-3}, the carbon deflagration may not lead to an explosion since electron capture is much faster at these high densities than at the lower densities encountered in the models of SN Ia. Moreover, if the central part of the white dwarf is in the solid state, the propagation mode of the burning front could be different. If the solid is strong enough, convection will be suppressed and the burning front will propagate as a *conductive* deflagration wave [5,6] though more study is needed on this point. The propagation velocity of a conductive deflagration wave is given approximately by the expression, $v_{def} \sim \delta/\tau_n \sim (\sigma/c_v\tau_n)^{1/2}$, where δ denotes the width of burning front, τ_n the nuclear burning timescale, σ the conductivity, and c_v the specific heat.[48,49] This gives $v_{def} \sim 100$ km s^{-1} at $\rho \sim 10^{10}$ g cm^{-3}, which is about 0.01 v_s.[49] Here v_s is the sound speed, equal to 1.0 - 1.3 $\times$ 10^4 km s^{-1} between $\rho = 10^9$ - 10^{10} g cm^{-3}.

Whether the white dwarf explodes or collapses depends on whether, behind the deflagration wave, nuclear energy release or electron capture is faster. A white dwarf whose mass is close to the Chandrasekhar mass has an adiabatic index close to 3, so that even a small energy release can cause substantial expansion.[49] However, a slight pressure decrease due to electron capture will easily induce collapse. If v_{def} is low (high) enough and/or the central density is high (low) enough, a carbon deflagration will lead to collapse (explosion). The outcome is rather sensitive to v_{def} and the central density.

The results of a numerical simulation of a conductive deflagration started at high central density ($\rho_c \simeq 10^{10}$ g cm^{-3}), with $\dot{M} = 2.5 \times 10^{-10}$ $M_\odot$ yr^{-1} and $M_{CO} = 1.16$ $M_\odot$, are shown in Figure 4. Here $X_C = X_O = 0.5$ and we have assumed that no chemical separation occurs. Pycnonuclear carbon burning commences in the solid region and turns into thermonuclear runaway as a result of the temperature rise. Throughout the simulation, convection is neglected.

The actual simulation of a conductive deflagration requires extremely fine zoning.[49] Instead of employing a grid whose fineness would slow the calculations unduly, we have parametrized the conductivity to obtain a range of reasonable v_{def}. With these, we have explored the range of possible hydrodynamical responses of the white dwarf. In Figure 7, the location of the deflagration front as a function of time, t, after initiation is plotted for three cases (A, B, C). In addition, Case D of the slowest propagation has been calculated. The average v_{def}/v_s for Cases A, B, C, and D is about 0.15, 0.1, 0.06, and 0,01, respectively. In Figure 8, the evolution of the central density, ρ_c, for Cases A - C is plotted.

4.2 Cases of Collapse

As Figure 8 indicates, in Case B, the central density *increases* as the deflagration front propagates outward. When the deflagration front has reached $M_r \simeq 0.9\ M_\odot$ ($t \simeq 0.6$ s), ρ_c is as high as 10^{11} g cm^{-3}. Clearly, the white dwarf now undergoes quasi-dynamic contraction (not yet free-fall collapse) because electron capture on NSE elements rapidly reduce the electron mole number, Y_e, behind the deflagration wave. This effect dominates the opposing effect of nuclear burning. In the central region of $\rho_c \simeq 10^{10}$ g cm^{-3}, typical values of τ_{ec} ($\equiv Y_e\ /|\dot{Y}_e|$) are 0.06 s and 0.16 s for $Y_e \simeq 0.5$ and 0.47, respectively. At $t =$ 0.16 s, Y_e has dropped to 0.42 at the center. Because of the decrease in the electron capture rate in the central region, electron capture is fastest at the deflagration front and thus the density there is important. In Case B, the density at the front is gradually decreasing but is still as high as 4×10^9 g cm^{-3} at $M_r = 0.9\ M_\odot$, and τ_{ec} is as short as $\simeq 0.3$ s (at $Y_e =$ 0.5). Moreover, once the contraction of the white dwarf begins, photodissociation becomes important, further promoting collapse.

In Case C, the contraction is much more gradual than in Case B because the deflagration wave is slower. When ρ_c reaches 10^{11} g cm^{-3}, the burned mass is only 0.13 $M_\odot$ (Figs. 7 and 8).

In Case D, for which v_{def} ($\sim 0.01\ v_s$) is close to the actual conductive deflagration speed, it takes 155 s to reach $\rho_c \simeq 10^{11}$ g cm^{-3}. At $t = 155$ s, the mass of the burned region is only 0.03 $M_\odot$ and $Y_e \sim 0.39$.

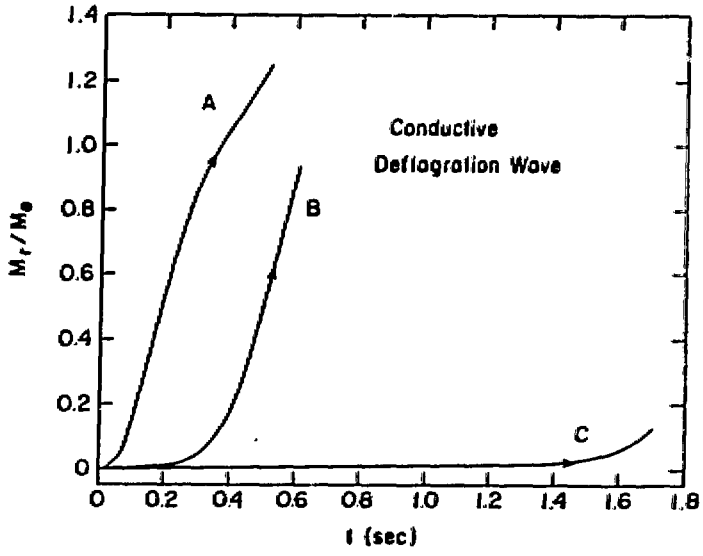

Figure 7: Propagation of the conductive deflagration wave. The location (M_r) of the deflagration front is shown as a function of time, t, for three cases (A, B, C) of parametrized conductivity.

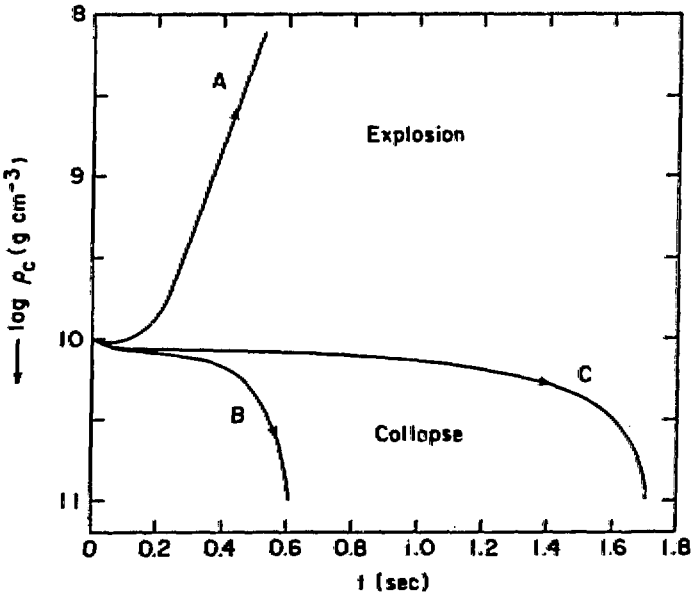

Figure 8: Change in the central density of the white dwarf associated with the propagation of the conductive deflagration wave. Relatively slow propagation in Cases B and C leads to the increase in ρ_c, i.e., collapse of the white dwarf. On the other hand, faster proapagation in Case A induces the explosion of the white dwarf.

4.3 Case of Explosion

On the other hand, in Case A, ρ_c decreases as the deflagration propagates outward. By the time the front has reached $M_r \simeq 1.2\ M_\odot$, the total energy of the white dwarf is already 1.2×10^{51} ergs and it is clear that it will be completely disrupted. Nuclear energy release dominates electron capture because the front's density, and hence its electron capture rate, decreases as the front propagates outward. The expansion of the burned core of the white dwarf decreases the density and temperature of the entire star. Once this expansion is substantial, it is impossible for electron capture to induce reimplosion. Only for initial central density as high as 3×10^{10} g cm^{-3},[11] similar to those in the detonation case, would reimplosion be a possible outcome.

Because of the expansion, when the deflagration front has reached $M_r = 1.0$ - $1.16\ M_\odot$, its density is as low as 10^6 - 10^7 g cm^{-3}. Therefore, some intermediate mass elements, such as Ca, Ar, S, and Si, are synthesized.[16] When the deflagration wave arrives at the base of helium layer ($M_r = 1.16\ M_\odot$), it turns into a helium *detonation* because helium has a large Q-value and a low ignition temperature. Despite the expansion of the white dwarf, detonation wave does not die and it processes most of the matter to ^{56}Ni. Were it not for the Ca - Si layer sandwiched between the two ^{56}Ni layers, the final outcome for Case A would be similar to the outcome for the double detonation supernovae,[41,42] where both carbon and helium layers are burned to ^{56}Ni. This type of supernovae should not be very frequent since they eject too much neutron-rich iron peak matter into the Galaxy.[24,50]

4.4 Convective Deflagration

If carbon ignition at high densities occurs for $\dot{M} > 4 \times 10^{-8}\ M_\odot$ yr^{-1} and $M_{CO} > 1.2\ M_\odot$, adiabatic compression may have already melted the solid core when carbon is ignited. Convective deflagration would then develope, though conductive deflagration could still dominate in the central region.[49] Even for the solid core, propagation of the deflagration wave is not necessarily due to conduction alone since convection could influence the melting the solid core.[51] To investigate these cases, a set of numerical experiments has been performed with the above model, but under the assumption that the deflagration

wave is propagating by convection in fluid layers. Our treatment of convection is the same as that employed by Nomoto et al.,[16] i.e., Unno's [52] time-dependent mixing length theory with a parameter $\alpha = \ell / H_p$ where ℓ is the mixing length and H_p is the pressure scale height.

For $\alpha = 0.7$, the propagation velocity is as slow as $v_{def}/v_s \sim 0.06$, 0.09, and 0.11 when the deflagration reaches $M_r/M_\odot = 0.2$, 0.4, and 0.6, respectively. As expected, the white dwarf collapses as in Case B. On the other hand, for $\alpha = 1.0$, $v_{def}/v_s \sim 0.10$, 0.15, and 0.20 at $M_r/M_\odot = 0.2$, 0.4, and 0.6, respectively, and the white dwarf explodes completely. Since a value for α of 0.7 is preferred in the low density carbon deflagration model of SN Ia (§3),[16] a plausible choice for α in the present context may be 0.7, not 1.0. (For both low and high central densities, the carbon deflagration with $\alpha = 1.0$ grows into a *detonation* in the outer layer and incinerates almost the entire star to the iron peak. This is incompatible with observations of SN Ia.[16]) Therefore, for plausible choices of the α parameter, a carbon deflagration initiated at high densities will result in white dwarf collapse, not explosion.

5. CONCLUDING REMARKS AND DISCUSSION

We have demonstrated that if a carbon deflagration is initiated in the center of the white dwarf when $\rho_c \simeq 10^{10}$ g cm^{-3} and if the propagation velocity of the deflagration wave is slower than a certain critical speed, v_{crit}, the outcome is collapse, not explosion. For $v_{def} > v_{crit}$, complete disruption results (and the ejecta contain too much neutron-rich matter). The value of v_{crit} depends on ρ_c at carbon ignition. For $\rho_c \simeq 1 \times 10^{10}$ g cm^{-3}, $v_{crit} \sim 0.15\ v_s$. A lower ρ_c implies a lower v_{crit}. Below a certain critical density (perhaps, $\sim 6 - 8 \times 10^9$ g cm^{-3}),[12] even extremely slow deflagrations results in explosions. In our case of $\rho_c \simeq 1 \times 10^{10}$ g cm^{-3}, for both conductive and convective deflagrations $v_{def} < v_{crit}$ and, therefore, collpase will result.

Such a high central density is reached in two regions of the $\dot{M}$ - M_{CO} plane of Figure 1. One is defined by $\dot{M} > 4 \times 10^{-8}\ M_\odot$ yr^{-1} and $M_{CO} > 1.2\ M_\odot$, while the other is defined by $\dot{M} < 10^{-9}\ M_\odot$ yr^{-1} and $M_{CO} > 1.13\ M_\odot$. The frequency of such systems

may be small. First, if hydrogen-rich matter accretes at $\dot{M} < 10^{-9}\ M_\odot\ \mathrm{yr}^{-1}$, nova-like explosions will prevent the white dwarf mass from growing.[53] The hydrogen flash can be avoided if the companion star is a helium star.[54,55] Secondly, massive C+O white dwarfs ($> 1.2\ M_\odot$) may be rare.[56] The formation of such white dwarfs might be prevented if the precursor star lost its hydrogen-rich envelope by either a stellar wind or Roche-lobe overflow before its degenerate C+O core could grow substantially.

As seen in Figure 2, the accretion-induced collapse is the outcome for a wider range of parameter space for O+Ne+Mg white dwarfs.[7] The initial mass of the white dwarf, M_{ONeMg}, is larger than $\sim 1.2\ M_\odot$.[9,57,58] In many cases, M_{ONeMg} is very close to the Chandrasekhar mass, so that only a small mass increase is enough to trigger collapse. However, an O+Ne+Mg white dwarf is formed from an 8 - 10 $M_\odot$ star.[57] The number of such systems may be significantly smaller than the number of systems containing C+O white dwarfs whose precursors are 1 - 8 $M_\odot$ stars, perhaps, by four order of magnitude.[44] Even so, the number of low mass X-ray binaries is much smaller than the number of SN I and the statistics may be consistent.[59]

A hydrodynamical calculation of such a white dwarf collapse has not been carried out. Its collapse should be similar to the collapse of the O+Ne+Mg cores of 8 - 10 $M_\odot$ stars,[60–62] but some differences are anticipated. In both classes of collapse, the white dwarf or the core contains nuclear fuel (C+O or O+Ne+Mg) which ignites during infall. Electron captures occur only in the NSE layer behind the burning front and, therefore, the region of small Y_e is confined to a central region which grows gradually. The collapse is slower than the collapse of the iron core of a massive star until the burning front has propagated to roughly $\sim 0.8\ M_\odot$.[60] Afterwards the collapse accerelates quickly. Y_e in the NSE region of collapsing white dwarf is smaller than Y_e in iron cores because the entropy at the burning front is high. These two effects result in a homologous core whose mass is smaller and an outer infalling layer which is less dense than is the case in iron core collpase.[60] Such a structure has two effects on the bounce shock. First, the binding energy of the rebounding core is smaller and, hence, the shock wave is initially weaker.[63,64] Secondly, the low density in the outer layers makes the shock propagation easier. Which effect dominates depends on the details of collapse hydrodynamics.

The location and propagation speed of the burning front may have important effects on the hydrodynamics. The initial composition and entropy of the collapsing star may be the determining factor. During collapse, nuclear burning is ignited when the temperature, which is increasing due to adiabatic compression, reaches the ignition temperature. If the white dwarf is composed of C+O, the ignition temperature and density for carbon are lower than for oxygen. At lower densities, effects of nuclear energy release is larger. On the other hand, a white dwarf has much lower entropy than a red-giant core. For lower entropy, the ignition of nuclear fuel is delayed until higher density is reached. Without calculating the collapse, we don't know whether mass is ejected.

Even if no mass is ejected, a neutron star will be formed because the residue's mass ($1.4\ M_\odot$ (baryon mass), $\sim 1.3\ M_\odot$ (gravitational mass)) is smaller than the maximum mass of a neutron star. Nevertheless, it is important to know whether some mass is ejected by the bounce shock and, if mass is ejected, what its composition is. If some ^{56}Ni is ejected, the white dwarf collapse can be observed as a *dim* Type I supernova. Otherwise, the collapse would be *silent*, because most of the explosion energy would go into the kinetic energy of expansion. The interior temperatures would be too low to produce a significant optical light curve. If the shock wave is strong enough, some neutron-rich species will be ejected. This might be an important site of some neutron-rich isotopes.[65,66] Mass ejection will affect the binary evolution after the explosion and the results can be compared to the observed neutron star binary systems.[4]

ACKNOWLEDGEMENT

It is a pleasure to thank Drs. S.H. Kahana, G.E. Brown, A. Yahil for useful discussion and hospitality during my stay in Brookhaven and Stony Brook. I would like to thank Dr. A. Burrows for the reading of the manuscript and comments. I also would like to thank Drs. D. Branch, J.C. Wheeler, and R. Harkness for informative discussion on Type I supernovae during my visit to Univ. of Oklahoma and Texas. This work has been supported in part by the U. S. Department of Energy under Contract No. DE-AC02-76CH00016.

REFERENCES

1) Nomoto, K. 1986, *Ann. New York Acad. Sci.*, *470*, 294.
2) Woosley, S.E., and Weaver, T.A. 1986, *Ann. Rev. Astr. Ap.*, in press.
3) Van den Heuvel, E.P.J. 1984, *J. Ap. Astr.*, *5*, 209.
4) Taam, R.E., and van den Heuvel, E.P.J. 1986, *Ap. J.*, *305*, 235.
5) Canal, R., and Isern, J. 1979, in *IAU Colloq. 53, White Dwarfs and Variable Degenerate Stars*, ed. H.M. Van Horn and V. Weidemann (Rochester: Univ. of Rochester), p.52.
6) Isern, J., Labay, J., Hernanz, M., and Canal, R. 1983, *Ap. J.*, *273*, 320.
7) Nomoto, K., Miyaji, S., Yokoi, K., and Sugimoto, D. 1979, in *IAU Colloq. 53, White Dwarfs and Variable Degenerate Stars*, ed. H.M. Van Horn and V. Weidmann (Rochester: Univ. of Rochester), p.56.
8) Miyaji, S., Nomoto, K., Yokoi, K., and Sugimoto, D. 1980, *Pub. Astr. Soc. Japan*, *32*, 303.
9) Nomoto, K. 1980, in *Type I Supernovae*, ed. J. C. Wheeler (Austin: Univ. of Texas), p. 164.
10) Mochkovitch, R. 1983, *Astr. Ap.*, *122*, 212.
11) Bruenn, S.W. 1972, *Ap. J. Suppl.*, *24*, 283.
Mazurek, T.J., Truran, J.W., and Cameron, A.G.W. 1974, *Ap. Space Sci.*, *27*, 261.
12) Ivanova, L.N., Imshennik, V.S., and Chechetkin, V.M. 1974, *Ap. Space Sci.*, *31*, 497.
13) Nomoto, K. 1982a, *Ap. J.*, *253*, 798.
14) Nomoto, K. 1984a, in *Stellar Nucleosynthesis*, ed. C. Chiosi and A. Renzini (Dordrecht: Reidel), p. 205.
15) Nomoto, K., and Iben, I. Jr. 1985, *Ap. J.*, *297*, 531.
Kawai, Y., Saio, H., and Nomoto. K. 1986, in preparation.
16) Nomoto, K., Thielemann, F.K., and Yokoi, K. 1984, *Ap. J.*, *286*, 644.
Thielemann, F.-K., Nomoto, K., and Yokoi, K. 1986, *Astr. Ap.*, *158*, 17.
17) Saio, H., and Nomoto, K. 1985, *Astr. Ap.*, *150*, L21.
18) Woosley. S .E., and Weaver, T.A. 1986b, in *Nucleosynthesis and Its Implications for Nuclear and Particle Physics*, ed. J. Audouze and T. van Thuan (Dordrecht: Reidel).
19) Canal, R. 1986, this volume.
20) Taam, R.E. 1980, *Ap. J.*, *242*, 749.
21) Fujimoto, M.Y., and Sugimoto, D 1982, *Ap. J.*, *257*, 291.
22) Woosley, S.E., Axelrod, R.S., and Weaver, T.A. 1984, in *Stellar Nucleosynthesis*, ed. C. Chiosi and A. Renzini (Dordrecht: Reidel), p.263.
23) Chevalier, R.A. 1981, *Ap. J.*, *246*, 267.
24) Sutherland, P., and Wheeler, J.C. 1984, *Ap. J.*, *280*, 282.
25) Branch, D., Lacy, C.H., McCall, M.L., Sutherland, P.G., Uomoto, A., Wheeler, J.C., and Wills, B.J. 1983, *Ap. J.*, *270*, 123.
26) Branch, D., Doggett, J.B., Nomoto, K, and Thielemann, F.-K. 1985, *Ap. J.*, *294*, 619.
27) Harkness, R.P. 1986, in *IAU Colloq. 89, Radiation Hydrodynamics in Stars and Compact Objects*, ed. D. Mihalas and K.H. Winkler (Dordrecht: Reidel), in press.
28) Wheeler, J.C., and Levreault, R. 1985, *Ap. J. (Letters)*, *294*, L17.
29) Uomoto, A., and Kirshner, R.P. 1985, *Astr. Ap.*, *149*, L7.
30) Elias, J.H., Mathews, K., Neugebauer, G., and Persson, S.E. 1985, *Ap. J.*, *296*, 379.
31) Panagia, N., Sramek, R.A., and Weiler, K.W. 1986, *Ap. J. (Letters)*, *300*, L15.
32) Gaskell, C.M., Cappellaro, E., Dinerste in, H., Garnett, D., Harkness, R.P., and Wheeler, J.C. 1986, *Ap. J.*, in press.

33) Filippenko, A.V., and Sargent, W.L.W. 1985, *Nature*, *316*, 407.
34) Begelman, M.C., and Sarazin, C.L. 1986, *Ap. J. (Letters)*, *302*, L59.
35) Chevalier, R.A. 1986, *Highlights of Astronomy*, in press.
36) Woosley, S.E. 1986, Saas-Fe Lecture Notes.
37) Branch, D. 1986 *Ap. J. (Letters)*, *300*, L51.
38) Branch, D., and Nomoto, K. 1986, *Astr. Ap.*, in press.
39) Wheeler, J.C., and Harkness, R. 1986, in *Distances of Galaxies and Deviations from the Hubble Flow*, ed. B.M. Madore and R.B. Tully (Dordrecht: Reidel), in press.
40) Branch, D., and Venkatakrishna, K.L. 1986, *Ap. J. (Letters)*, in press.
41) Nomoto, K. 1982b, *Ap. J.*, *257*, 780.
42) Woosley, S.E., Taam, R.E., and Weaver, T.A. 1986, *Ap. J.*, *301*, 601.
43) Davidson, K., and Ostriker, J.P. 1973, *Ap. J.*, *179*, 585.
44) Iben, I. Jr., and Tutukov, A.V. 1984, *Ap. J. Suppl.*, *54*, 335.
45) Sramek, R.A., Panagia, N., and Weiler, K.W. 1984, *Ap. J. (Letters)*, *285*, L59.
46) Chevalier, R.A. 1984, *Ap. J. (Letters)*, *285*, L63.
47) Branch, D., and Doggett, J.B. 1985, *A. J.*, *270*, 2218.
48) Buchler, J.R., Colgate, S.A., and Mazurek, T.J. 1980, *Colloq. C2, suppl. 3*, *41*, C2-159.
49) Woosley, S.E., and Weaver, T.A. 1986c, in *IAU Colloq. 89, Radiation Transport and Hydrodynamics*, ed. D. Mihalas and K.H. Winkler (Dordrecht: Reidel), in press.
50) Nomoto, K., Thielemann, F.-K., and Wheeler, J.C. 1984, *Ap. J. (Letters)*, *279*, L23.
51) Mochkovitch, R. 1980, *Thesis*, University of Paris.
52) Unno, W. 1967, *Pub. Astr. Soc. Japan*, *19*, 140.
53) MacDonald, J. 1984, *Ap. J.*, *283*, 241.
54) Savonije, G.J., de Kool, M., and van den Heuvel, E.P.J. 1986, *Astr. Ap.*, *155*, 51.
55) Iben, I. Jr., and Tutukov, A. 1986, *Ap. J.*, submitted.
56) Law, W.Y., and Ritter, H. 1983, *Astr. Ap.*, *123*, 33.
57) Nomoto, K. 1984c, *Ap. J.*, *277*, 791.
58) Nomoto, K. 1984d, in *Problems of Collapse and Numerical Relativity*, ed. D. Bancel and M. Signore (Dordrecht: Reidel), p.89.
59) Webbink, R.F. Rappaport, S., and Savonije, G.J. 1983, *Ap. J.*, *270*, 678.
60) Hillebrandt, W., Nomoto, K., and Wolff, R.G. 1984, *Astr. Ap.*, *133*, 175.
Hillebrandt, W. *Ann. New York Acad. Sci.*, *422*, 197.
61) Burrows, A., and Lattimer, J.M. 1985, *Ap. J. (Letters)*, *299*, L19.
62) Baron, E., Cooperstein, J., and Kahana, S.H. 1986, private communication.
63) Brown, G.E., Bethe, H.A., Baym, G. 1982, *Nucl. Phys.*, *A375*, 481.
64) Lattimer, J.M., Burrows, A., and Yahil, A 1985, *Ap. J.*, *288*, 644.
65) Hartmann, D., Woosley, S.E., and El Eid, M.F. 1985, *Ap. J.*, *297*, 837.
66) Takahashi, Y., Miyaji, S., Parnell, T.A., Weisskopf, M.C., Hayashi, T. and Nomoto, K. 1986, *Nature*, in press.

DISCLAIMER